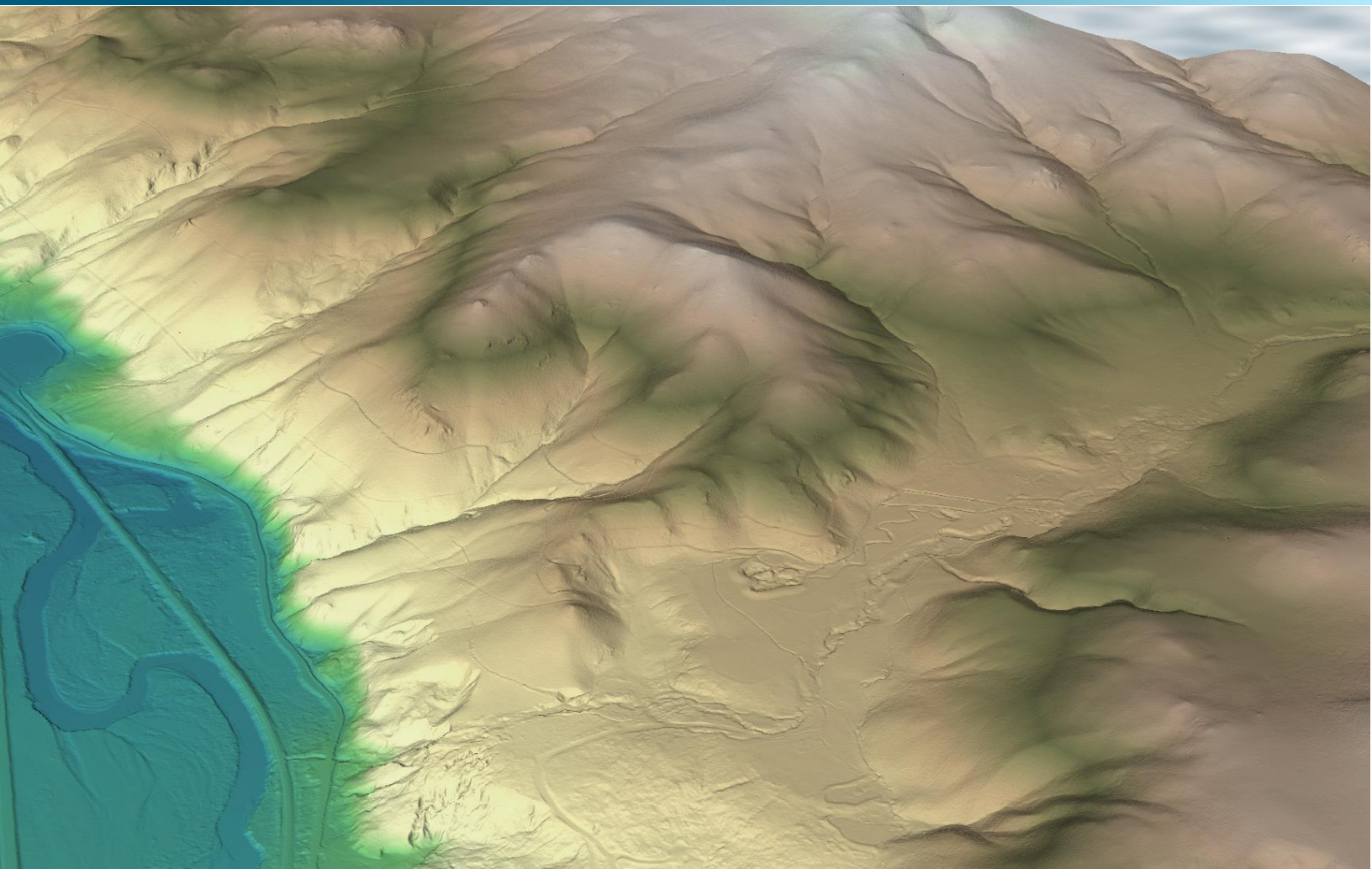


May 27, 2016



Dillon AOI, Beaverhead County LiDAR Technical Data Report



The Montana Department of
Natural Resources
& Conservation

Steve Story

Montana Dept. of Natural Resources & Conservation
1424 9th Avenue
Helena, MT 59620-1601
PH: 406-444-6816



QSI Corvallis

517 SW 2nd St., Suite 400
Corvallis, OR 97333
PH: 541-752-1204

TABLE OF CONTENTS

- INTRODUCTION 1
 - Deliverable Products 2
- ACQUISITION 4
 - Planning..... 4
 - Airborne LiDAR Survey 5
 - Ground Control..... 6
 - Monumentation 6
 - Ground Survey Points (GSPs)..... 7
- PROCESSING 9
 - LiDAR Data..... 9
 - Feature Extraction..... 11
 - Hydro-flattening and Water’s edge breaklines 11
 - Contours 12
- RESULTS & DISCUSSION..... 13
 - LiDAR Density 13
 - LiDAR Accuracy Assessments 16
 - LiDAR Non-Vegetated Vertical Accuracy 16
 - LiDAR Vegetated Vertical Accuracy 18
 - LiDAR Relative Vertical Accuracy 19
- SELECTED IMAGES..... 20
- GLOSSARY 22
- APPENDIX A - ACCURACY CONTROLS 23

Cover Photo: A view looking east from the southern end of the Dillon AOI. The image was created from the LiDAR bare earth model colored by elevation.

INTRODUCTION

This photo taken by QSI acquisition staff shows a view of the location of QSI's BEAV_01 monument, established within the Dillon AOI.



In late 2015, Quantum Spatial (QSI) was contracted by the Montana Department of Natural Resources & Conservation (MDNRC) to collect Light Detection and Ranging (LiDAR) data in the spring of 2016 for the Beaverhead County LiDAR project in Montana. The Beaverhead County project encompasses two sites: the Harlowton, Montana area of interest (AOI) and the Dillon, Montana AOI. QSI provided the Harlowton, Montana LiDAR delivery to MDNRC on January 27, 2016. This subsequent delivery provides LiDAR data acquired for the Dillon AOI only, and thereby concludes the contracted project agreement. Data were collected to aid MDNRC in assessing the topographic and geophysical properties of the area in order to facilitate floodplain mapping and hazard assessment.

This report accompanies the delivered LiDAR data for the Dillon, Montana AOI in Beaverhead County and documents contract specifications, data acquisition procedures, processing methods, and analysis of the final dataset including LiDAR accuracy and density. Acquisition dates and acreage are shown in Table 1, a complete list of contracted deliverables provided to MDNRC is shown in Table 2, and the project extent is shown in Figure 1.

Table 1: Acquisition dates, acreage, and data types collected on the Dillon AOI site

Project Site	Contracted Acres	Buffered Acres	Acquisition Dates	Data Type
Dillon AOI	37,620	39,962	04/04/2016, 04/07/2016	High resolution LiDAR

Deliverable Products

Table 2: Products delivered to the MDNRC for the Dillon AOI

Dillon, Montana Products Projection: UTM Zone 12 North Horizontal Datum: NAD83 (2011) Vertical Datum: NAVD88 (GEOID 12A) Units: Meters	
Points	LAS v 1.4 <ul style="list-style-type: none"> • All Returns • Raw Calibrated Flightline Swaths
Rasters	1.0 Meter Bare Earth Model <ul style="list-style-type: none"> • Hydro-flattened Bare Earth Model (ESRI Grid) • Hydro-flattened Bare Earth Model (ESRI Geodatabase) • Hydro-flattened Bare Earth Model (ASCII format)
Vectors	Shapefiles (*.shp) <ul style="list-style-type: none"> • Site Boundary • LiDAR Tile Index • Flightline Index • DEM Tile Index • Contours (0.5 m) • Ground Control and Check Points • Water Mask (3D Polygon Z) CAD Format <ul style="list-style-type: none"> • Water Mask (*.dxf) ESRI Geodatabase (*.gdb) <ul style="list-style-type: none"> • Contours (0.5 m)

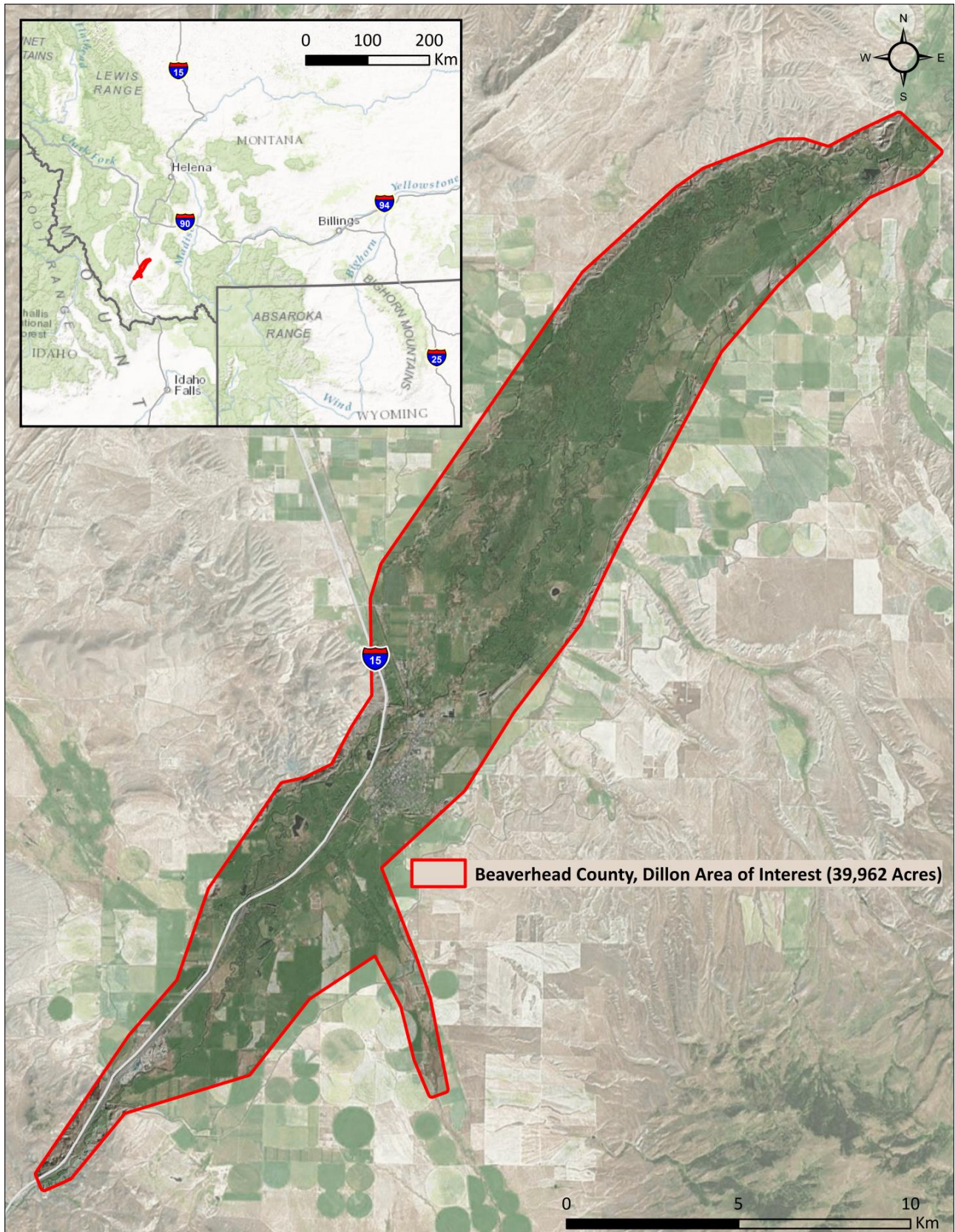


Figure 1: Location map of the Dillon AOI site in Montana

QSI's Cessna Caravan



Planning

In preparation for data collection, QSI reviewed the project area and developed a specialized flight plan to ensure complete coverage of the Dillon AOI LiDAR study area at the target point density of ≥ 8.0 points/m². Acquisition parameters including orientation relative to terrain, flight altitude, pulse rate, scan angle, and ground speed were adapted to optimize flight paths and flight times while meeting all contract specifications.

Factors such as satellite constellation availability and weather windows must be considered during the planning stage. Any weather hazards or conditions affecting the flights were continuously monitored due to their potential impact on the daily success of airborne and ground operations. In addition, logistical considerations including private property access and potential air space restrictions were reviewed.

Airborne LiDAR Survey

The LiDAR survey was accomplished using a Leica ALS80 system mounted in a Cessna Caravan 208. Table 3 summarizes the settings used to yield an average pulse density of ≥ 8 pulses/m² over the Dillon AOI. The Leica ALS80 laser system can record unlimited range measurements (returns) per pulse; however, it is not uncommon for some types of surfaces (e.g., dense vegetation or water) to return fewer pulses to the LiDAR sensor than the laser originally emitted. The discrepancy between first return and overall delivered density will vary depending on terrain, land cover, and the prevalence of water bodies. All discernible laser returns were processed for the output dataset.

Table 3: LiDAR specifications and survey settings

LiDAR Survey Settings & Specifications	
Acquisition Dates	04/04/2016, 04/07/2016
Aircraft Used	Cessna Caravan 208
Sensor	Leica ALS80
Survey Altitude (AGL)	1,800 m
Swath Width	965 m
Target Pulse Rate	310.8 kHz
Pulse Mode	Multiple Pulse in Air (2PiA)
Laser Pulse Diameter	39.6 cm
Mirror Scan Rate	58.4 Hz
Field of View	30°
GPS Baselines	≤ 13 nm
GPS PDOP	≤ 3.0
GPS Satellite Constellation	≥ 6
Maximum Returns	Unlimited
Intensity	8-bit, scaled to 16-bit
Resolution/Density	Average 8 pulses/m ²
Accuracy	RMSE _z ≤ 15 cm



Leica ALS80 LiDAR sensor

All areas were surveyed with an opposing flight line side-lap of $\geq 50\%$ ($\geq 100\%$ overlap) in order to reduce laser shadowing and increase surface laser painting. To accurately solve for laser point position (geographic coordinates x, y and z), the positional coordinates of the airborne sensor and the attitude of the aircraft were recorded continuously throughout the LiDAR data collection mission. Position of the aircraft was measured twice per second (2 Hz) by an onboard differential GPS unit, and aircraft attitude was measured 200 times per second (200 Hz) as pitch, roll and yaw (heading) from an onboard inertial measurement unit (IMU). To allow for post-processing correction and calibration, aircraft and sensor position and attitude data are indexed by GPS time.

Ground Control

Ground control surveys, including monumentation and ground survey points (GSPs), were conducted to support the airborne acquisition. Ground control data were used to geospatially correct the aircraft positional coordinate data and to perform quality assurance checks on final LiDAR data.



QSI-Established Monument
BEAV_01

Monumentation

The spatial configuration of ground survey monuments provided redundant control within 13 nautical miles of the mission areas for LiDAR flights. Monuments were also used for collection of ground survey points using real time kinematic (RTK) survey techniques.

Monument locations were selected with consideration for satellite visibility, field crew safety, and optimal location for GSP coverage. QSI established two new monuments for the Dillon AOI LiDAR project (Table 4, Figure 2). New monumentation was set using 5/8" x 30" rebar topped with stamped 2 ½ " aluminum caps. QSI's professional land surveying staff oversaw the establishment of all monuments.

Table 4: Monuments established for the Dillon AOI acquisition. Coordinates are on the NAD83 (2011) datum, epoch 2010.00.

Monument ID	Latitude	Longitude	Ellipsoid (meters)
BEAV_01	45° 16' 04.22336"	-112° 38' 30.17063"	1524.916
BEAV_02	45° 14' 39.38963"	-112° 35' 23.87876"	1526.372

To correct the continuously recorded onboard measurements of the aircraft position, QSI concurrently conducted multiple static Global Navigation Satellite System (GNSS) ground surveys (1 Hz recording frequency) over each monument. During post-processing, the static GPS data were triangulated with nearby Continuously Operating Reference Stations (CORS) using the Online Positioning User Service (OPUS¹) for precise positioning. Multiple independent sessions over the same monument were processed to confirm antenna height measurements and to refine position accuracy.

Monuments were established according to the national standard for geodetic control networks, as specified in the Federal Geographic Data Committee (FGDC) Geospatial Positioning Accuracy Standards for geodetic networks.² This standard provides guidelines for classification of monument quality at the 95% confidence interval as a basis for comparing the quality of one control network to another. The monument rating for this project is shown in Table 5.

¹ OPUS is a free service provided by the National Geodetic Survey to process corrected monument positions. <http://www.ngs.noaa.gov/OPUS>.

² Federal Geographic Data Committee, Geospatial Positioning Accuracy Standards (FGDC-STD-007.2-1998). Part 2: Standards for Geodetic Networks, Table 2.1, page 2-3. <http://www.fgdc.gov/standards/projects/FGDC-standards-projects/accuracy/part2/chapter2>

Table 5: Federal Geographic Data Committee monument rating for network accuracy

Direction	Rating
1.96 * St Dev _{NE} :	0.010 m
1.96 * St Dev _z :	0.010 m

For the Dillon AOI LiDAR project, the monument coordinates contributed no more than 1.4 cm of positional error to the geolocation of the final ground survey points and LiDAR, with 95% confidence.

Ground Survey Points (GSPs)

Ground survey points were collected using real time kinematic survey techniques. A Trimble R7 base unit was positioned at a nearby monument to broadcast a kinematic correction to a roving Trimble R10 GNSS receiver. All GSP measurements were made during periods with a Position Dilution of Precision (PDOP) of ≤ 3.0 with at least six satellites in view of the stationary and roving receivers. When collecting RTK data, the rover records data while stationary for five seconds, then calculates the pseudorange position using at least three one-second epochs. Relative errors for any GSP position must be less than 1.5 cm horizontal and 2.0 cm vertical in order to be accepted. See Table 6 for Trimble unit specifications.

GSPs were collected in areas where good satellite visibility was achieved on paved roads and other hard surfaces such as gravel or packed dirt roads. GSP measurements were not taken on highly reflective surfaces such as center line stripes or lane markings on roads due to the increased noise seen in the laser returns over these surfaces. GSPs were collected within as many flightlines as possible; however the distribution of GSPs depended on ground access constraints and monument locations and may not be equitably distributed throughout the study area (Figure 2).

Table 6: Trimble equipment identification

Receiver Model	Antenna	OPUS Antenna ID	Use
Trimble R7 GNSS	Zephyr GNSS Geodetic Model 2 RoHS	TRM57971.00	Static
Trimble R10	Integrated Antenna R10	TRMR10	Rover

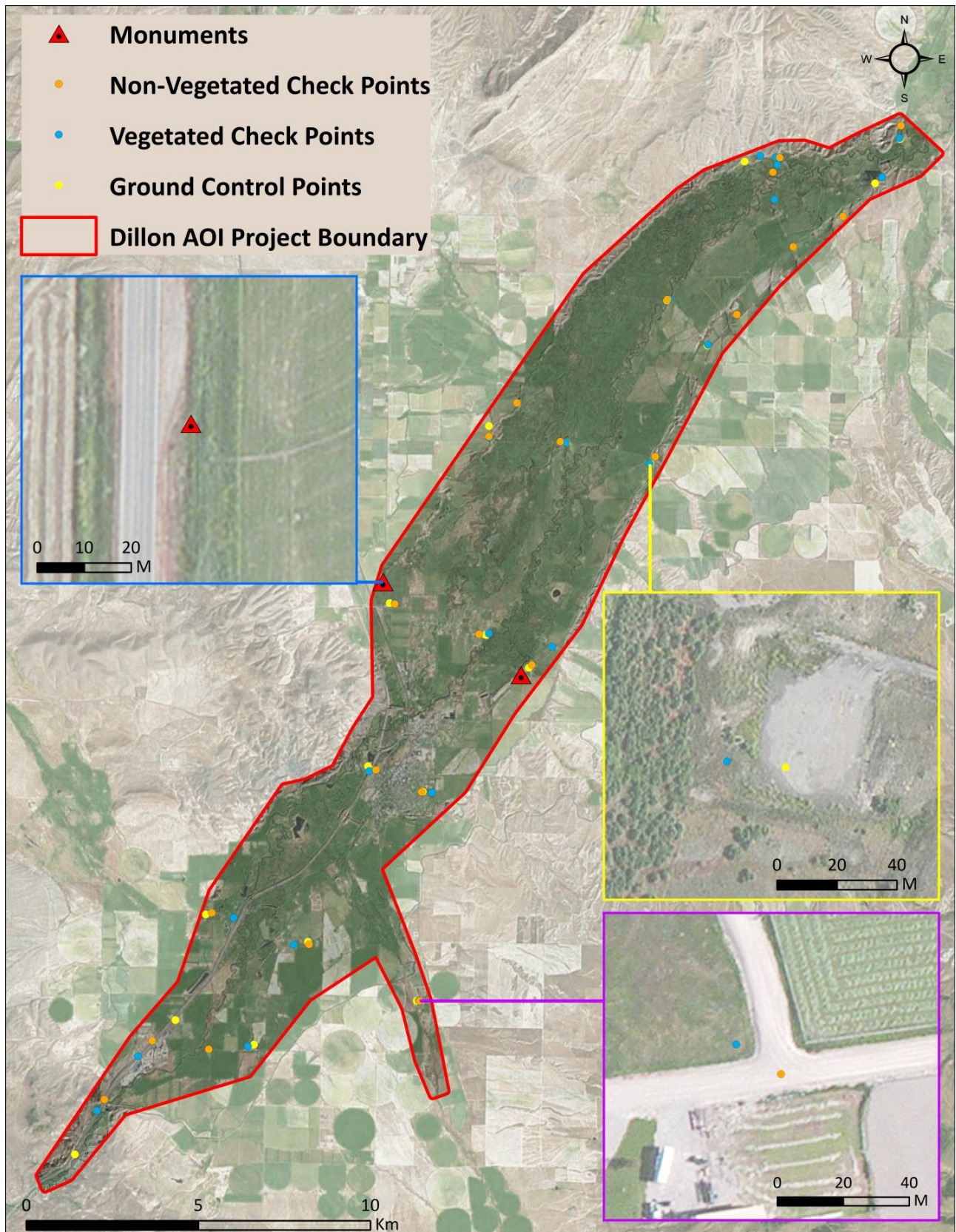
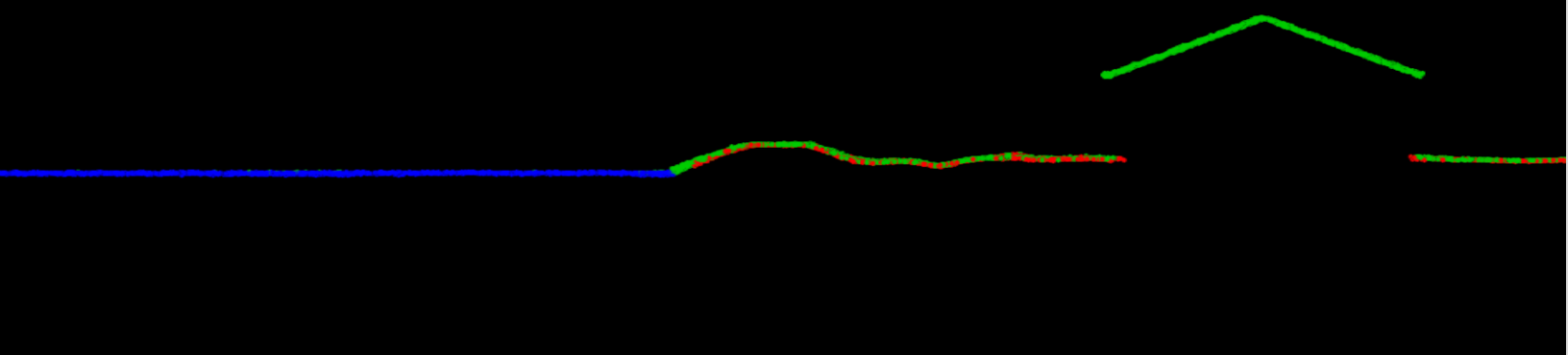


Figure 2: Ground survey location map

PROCESSING

Default ■
 Ground ■
 Water ■

This 2 meter LiDAR cross section shows a view of the Dillon AOI landscape, colored by point classification.



LiDAR Data

Upon completion of data acquisition, QSI processing staff initiated a suite of automated and manual techniques to process the data into the requested deliverables. Processing tasks included GPS control computations, smoothed best estimate trajectory (SBET) calculations, kinematic corrections, calculation of laser point position, sensor and data calibration for optimal relative and absolute accuracy, and LiDAR point classification (Table 7). Processing methodologies were tailored for the landscape. Brief descriptions of these tasks are shown in Table 8.

Table 7: ASPRS LAS classification standards applied to the Dillon AOI dataset

Classification Number	Classification Name	Classification Description
1	Default/Unclassified	Laser returns that are not included in the ground class, composed of vegetation and man-made structures
2	Ground	Laser returns that are determined to be ground using automated and manual cleaning algorithms
7	Noise	Laser returns that are often associated with birds, scattering from reflective surfaces, or artificial points below the ground surface
9	Water	Laser returns that are determined to be water using automated and manual cleaning algorithms
10	Ignored Ground	Ground points proximate to water's edge breaklines; ignored for correct model creation
11	Withheld	Laser returns that have intensity values of 0 or 255

Table 8: LiDAR processing workflow

LiDAR Processing Step	Software Used
Resolve kinematic corrections for aircraft position data using kinematic aircraft GPS and static ground GPS data. Develop a smoothed best estimate of trajectory (SBET) file that blends post-processed aircraft position with sensor head position and attitude recorded throughout the survey.	Waypoint Inertial Explorer v.8.6
Calculate laser point position by associating SBET position to each laser point return time, scan angle, intensity, etc. Create raw laser point cloud data for the entire survey in *.las (ASPRS v. 1.2) format. Convert data to orthometric elevations by applying a geoid12a correction.	Waypoint Inertial Explorer v.8.6 Leica Cloudpro v. 1.2.2
Import raw laser points into manageable blocks (less than 500 MB) to perform manual relative accuracy calibration and filter erroneous points. Classify ground points for individual flight lines.	TerraScan v.16
Using ground classified points per each flight line, test the relative accuracy. Perform automated line-to-line calibrations for system attitude parameters (pitch, roll, heading), mirror flex (scale) and GPS/IMU drift. Calculate calibrations on ground classified points from paired flight lines and apply results to all points in a flight line. Use every flight line for relative accuracy calibration.	TerraMatch v.16
Classify resulting data to ground and other client designated ASPRS classifications (Table 7). Assess statistical absolute accuracy via direct comparisons of ground classified points to ground control survey data.	TerraScan v.16 TerraModeler v.16
Generate bare earth models as triangulated surfaces. Export all surface models as ESRI GRIDs, ESRI Geodatabase, and ASCII format at a 1 meter pixel resolution.	TerraScan v.16 TerraModeler v.156 ArcMap v. 10.2.2

Feature Extraction

Hydro-flattening and Water's edge breaklines

Water bodies within the Dillon AOI were flattened to a consistent water level. These include lakes and other closed water bodies with a surface area greater than 2 acres. The hydro-flattening process eliminates artifacts in the digital terrain model caused by both increased variability in ranges or dropouts in laser returns due to the low reflectivity of water.

Hydro-flattening of closed water bodies was performed through a combination of automated and manual detection and adjustment techniques designed to identify water boundaries and water levels. Boundary polygons were developed using an algorithm which weights LiDAR-derived slopes, intensities, and return densities to detect the water's edge. The water edges were then manually reviewed and edited as necessary.

Once polygons were developed the initial ground classified points falling within water polygons were reclassified as water points to omit them from the final ground model. Elevations were then obtained from the filtered LiDAR returns to create the final breaklines and lakes were assigned a consistent elevation for an entire polygon within these breaklines.

Water boundary breaklines were then incorporated into the hydro-flattened DEM by enforcing triangle edges (adjacent to the breakline) to the elevation values of the breakline. This implementation corrected interpolation along the hard edge. Water surfaces were obtained from a TIN of the 3-D water edge breaklines resulting in the final hydro-flattened model (Figure 3).

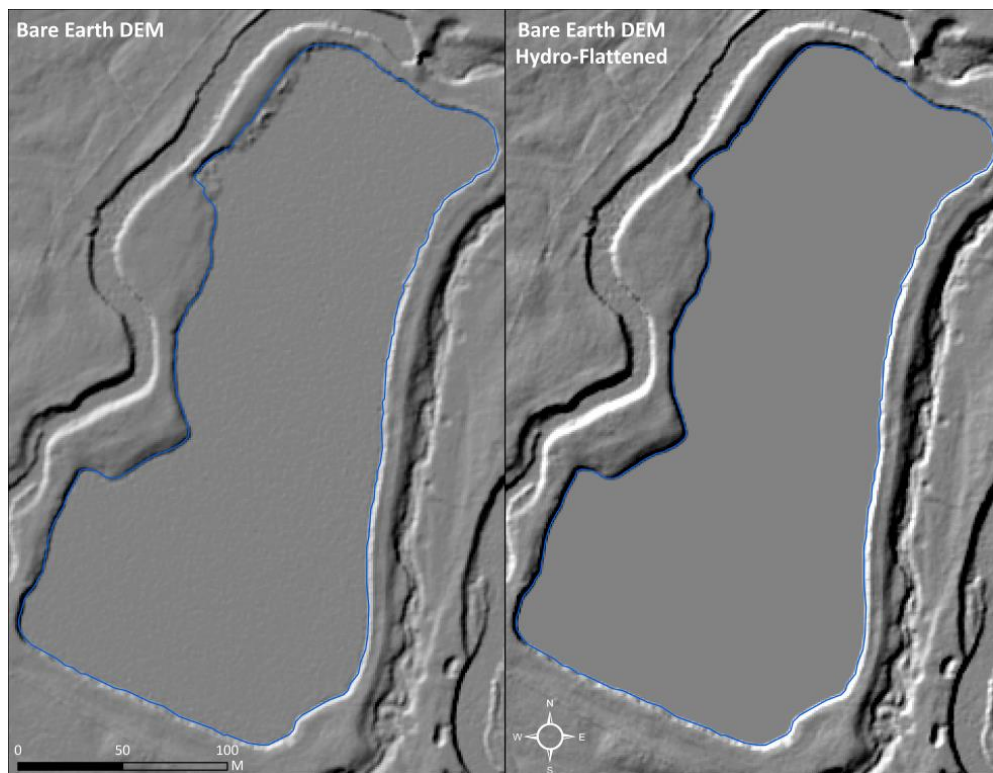


Figure 3: Example of hydro-flattening in the Dillon AOI LiDAR dataset

Contours

Contour generation from LiDAR point data required a thinning operation in order to reduce contour sinuosity. The thinning operation reduced point density where topographic change is minimal (i.e., flat surfaces) while preserving resolution where topographic change was present. Model key points were selected from the ground model every 20 feet with the spacing decreased in regions with high surface curvature. Generation of model key points eliminated redundant detail in terrain representation, particularly in areas of low relief, and provided for a more manageable dataset. Contours were produced through TerraModeler by interpolating between the model key points at even elevation increments.

Elevation contour lines were then intersected with ground point density rasters and a confidence field was added to each contour line. Contours which crossed areas of high point density have high confidence levels, while contours which crossed areas of low point density have low confidence levels. Areas with low ground point density are commonly beneath buildings and bridges, in locations with dense vegetation, over water, and in other areas where laser penetration to the ground surface was impeded (Figure 4).

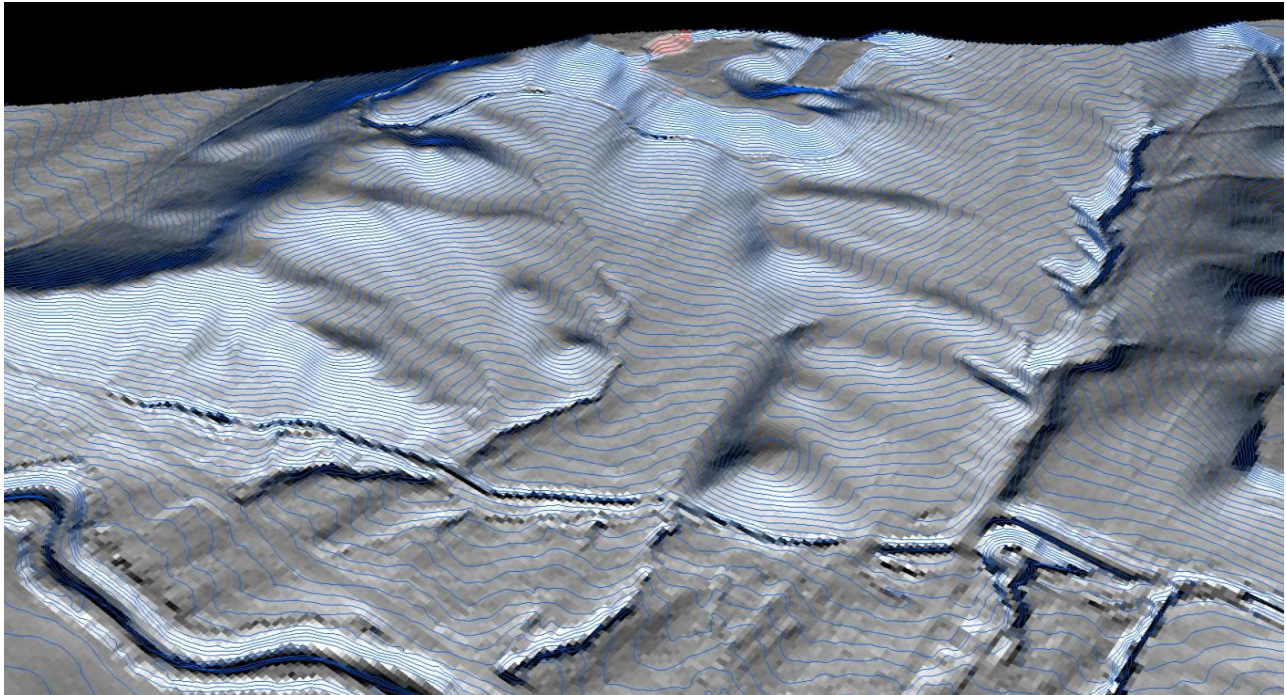
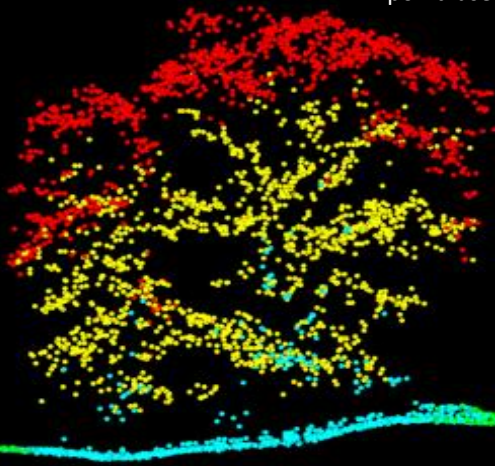


Figure 4: Contours draped over the Dillon AOI bare earth elevation model. Blue contours represent high confidence while the red contours represent low confidence.

Only Echo ■
 First of Many ■
 Intermediate ■
 Last of Many ■

This 2 meter LiDAR cross section shows a view of vegetation and bare ground in the Dillon AOI, colored by point laser echo.



LiDAR Density

The acquisition parameters were designed to acquire an average first-return density of 8 points/m². First return density describes the density of pulses emitted from the laser that return at least one echo to the system. Multiple returns from a single pulse were not considered in first return density analysis. Some types of surfaces (e.g., breaks in terrain, water and steep slopes) may have returned fewer pulses than originally emitted by the laser. First returns typically reflect off the highest feature on the landscape within the footprint of the pulse. In forested or urban areas the highest feature could be a tree, building or power line, while in areas of unobstructed ground, the first return will be the only echo and represents the bare earth surface.

The density of ground-classified LiDAR returns was also analyzed for this project. Terrain character, land cover, and ground surface reflectivity all influenced the density of ground surface returns. In vegetated areas, fewer pulses may penetrate the canopy, resulting in lower ground density.

The average first-return density of LiDAR data for the Dillon AOI was 11.09 points/m² while the average ground classified density was 6.95 points/m² (Table 9). The statistical and spatial distributions of first return densities and classified ground return densities per 100 m x 100 m cell are portrayed in Figure 5 through Figure 7.

Table 9: Average LiDAR point densities

Classification	Point Density
First-Return	11.09 points/m ²
Ground Classified	6.95 points/m ²

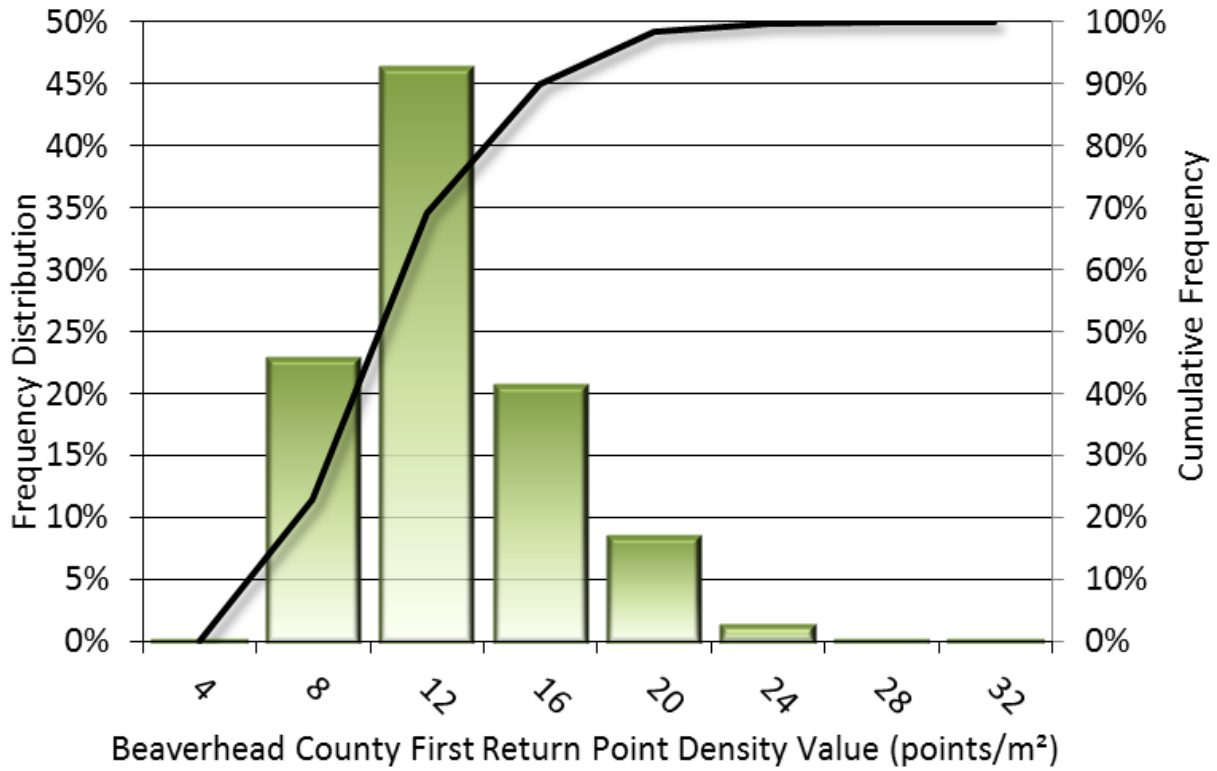


Figure 5: Frequency distribution of first return point density values per 100 x 100 m cell

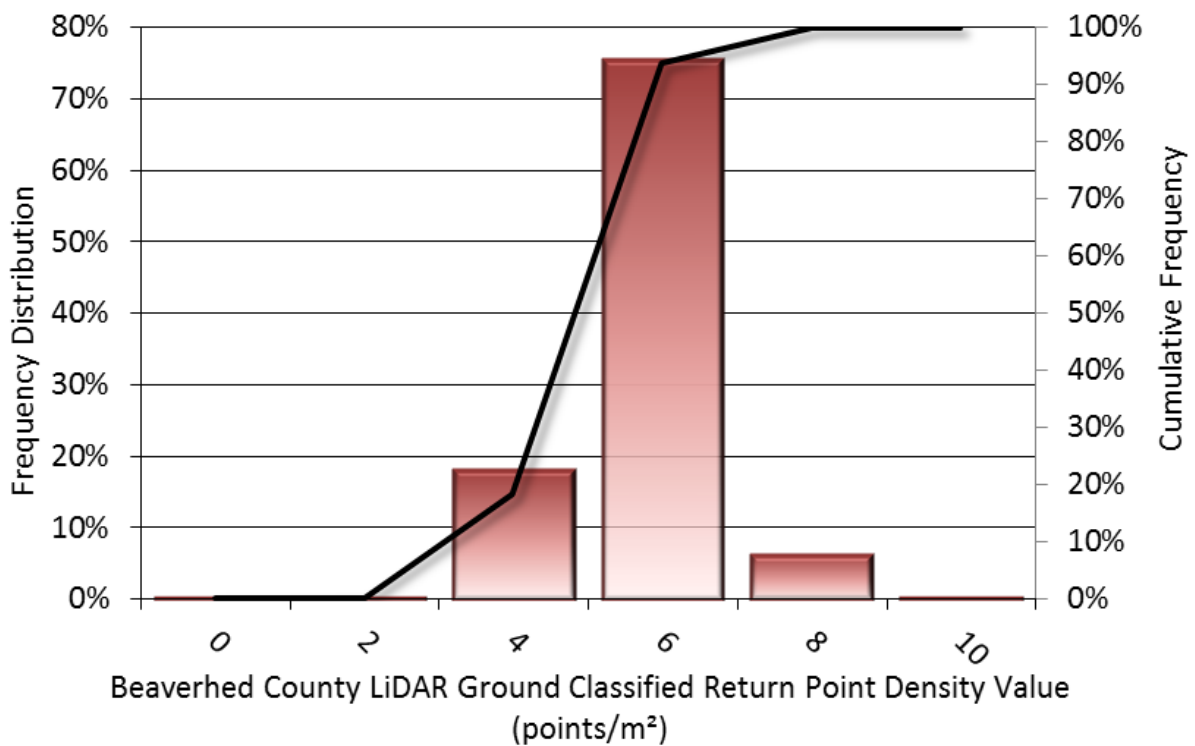


Figure 6: Frequency distribution of ground-classified return point density values per 100 x 100 m cell

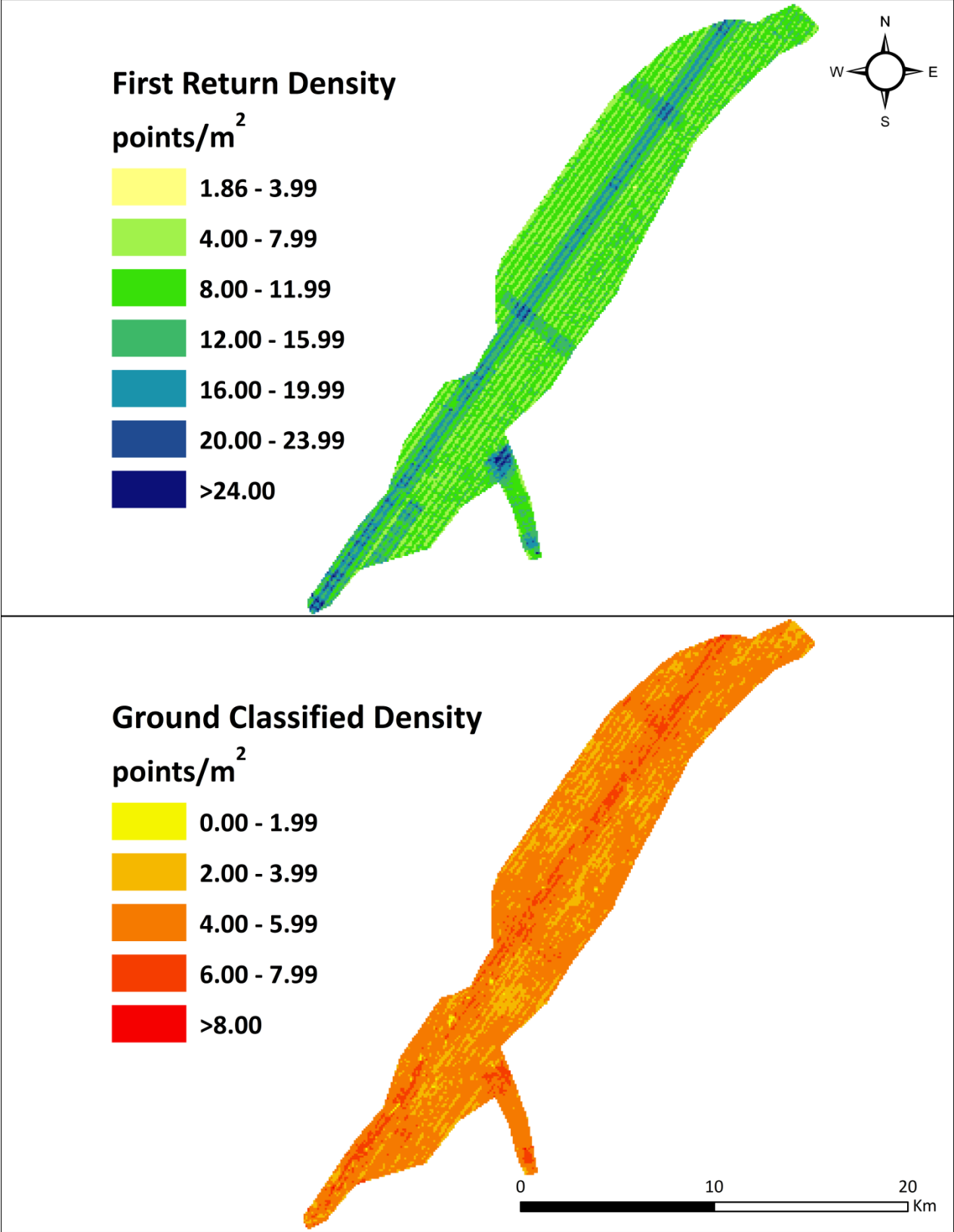


Figure 7: First return and ground-classified point density map for the Dillon AOI (100 m x 100 m cells)

LiDAR Accuracy Assessments

The accuracy of the LiDAR data collection can be described in terms of absolute accuracy (the consistency of the data with external data sources) and relative accuracy (the consistency of the dataset with itself). See Appendix A for further information on sources of error and operational measures used to improve relative accuracy.

LiDAR Non-Vegetated Vertical Accuracy

Non-Vegetated Vertical Accuracy (NVA) was assessed according to guidelines presented in the FGDC National Standard for Spatial Data Accuracy³. NVA compares known ground quality assurance point data collected on open, bare earth surfaces with level slope (<20°) to the triangulated surface generated by the LiDAR points. NVA is a measure of the accuracy of LiDAR point data in open areas where the LiDAR system has a high probability of measuring the ground surface and is evaluated at the 95% confidence interval (1.96 * RMSE), as shown in Table 10.

The mean and standard deviation (sigma σ) of divergence of the ground surface model from ground check point coordinates are also considered during accuracy assessment. These statistics assume the error for x, y, and z is normally distributed, and therefore the skew and kurtosis of distributions are also considered when evaluating error statistics. For the Dillon AOI survey, 22 ground check points were withheld in total resulting in a non-vegetated vertical accuracy of 0.029 meters (Figure 8).

Table 10: NVA results

Absolute Accuracy	
Sample	22 points
NVA (1.96*RMSE)	0.029 m
Average	-0.003 m
Median	-0.010 m
RMSE	0.015 m
Standard Deviation (1 σ)	0.015 m

³ Federal Geographic Data Committee, ASPRS POSITIONAL ACCURACY STANDARDS FOR DIGITAL GEOSPATIAL DATA EDITION 1, Version 1.0, NOVEMBER 2014. <http://www.asprs.org/PAD-Division/ASPRS-POSITIONAL-ACCURACY-STANDARDS-FOR-DIGITAL-GEOSPATIAL-DATA.html>.

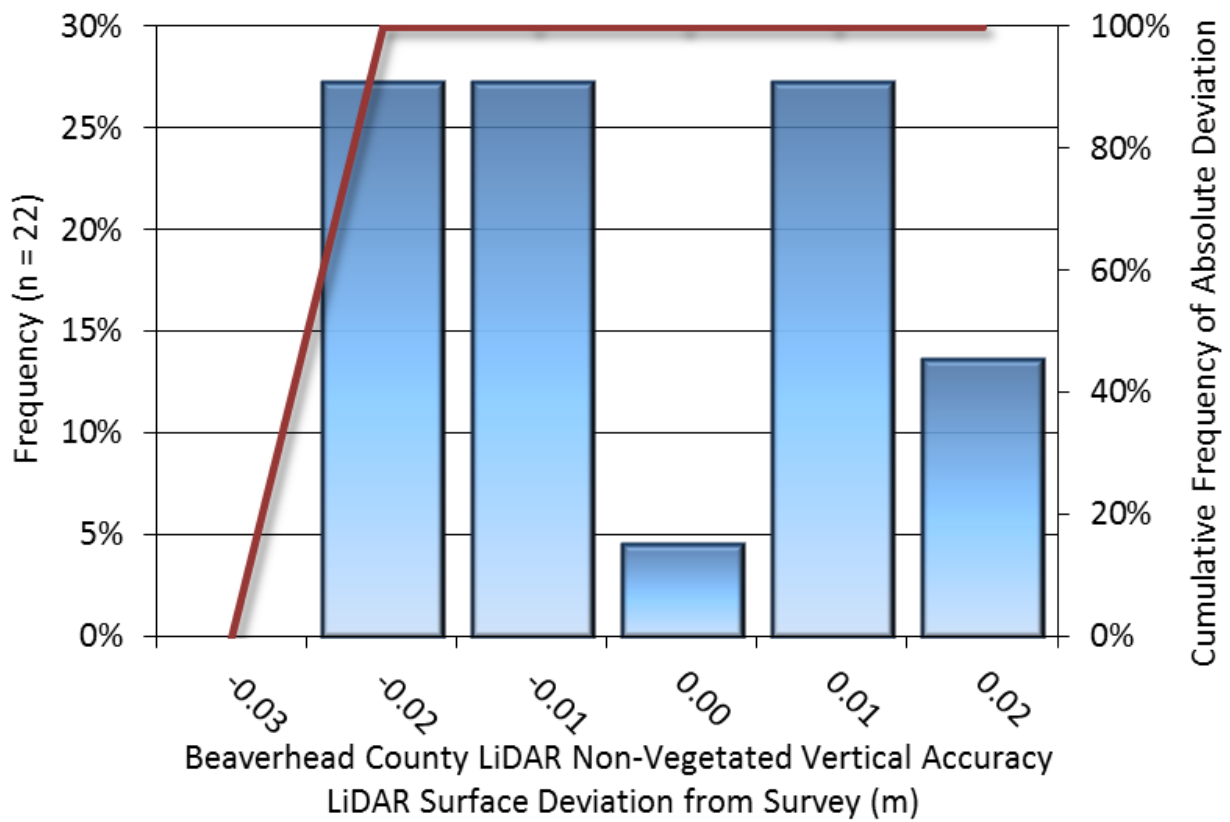


Figure 8: Frequency histogram for LiDAR surface deviation from ground check point values

LiDAR Vegetated Vertical Accuracy

QSI also assessed vertical accuracy using Vegetated Vertical Accuracy (VVA) reporting. VVA compares known ground quality assurance point data collected over vegetated surfaces using land class descriptions to the triangulated ground surface generated by the ground classified LiDAR points. VVA is evaluated at the 95th percentile (Table 11, Figure 9).

Table 11: Vegetated Vertical Accuracy for the Dillon AOI Project

Vegetated Vertical Accuracy (VVA)	
Sample	22 points
Average Dz	0.031 m
Median	0.025 m
RMSE	0.047 m
Standard Deviation (1σ)	0.035 m
95 th Percentile	0.080 m

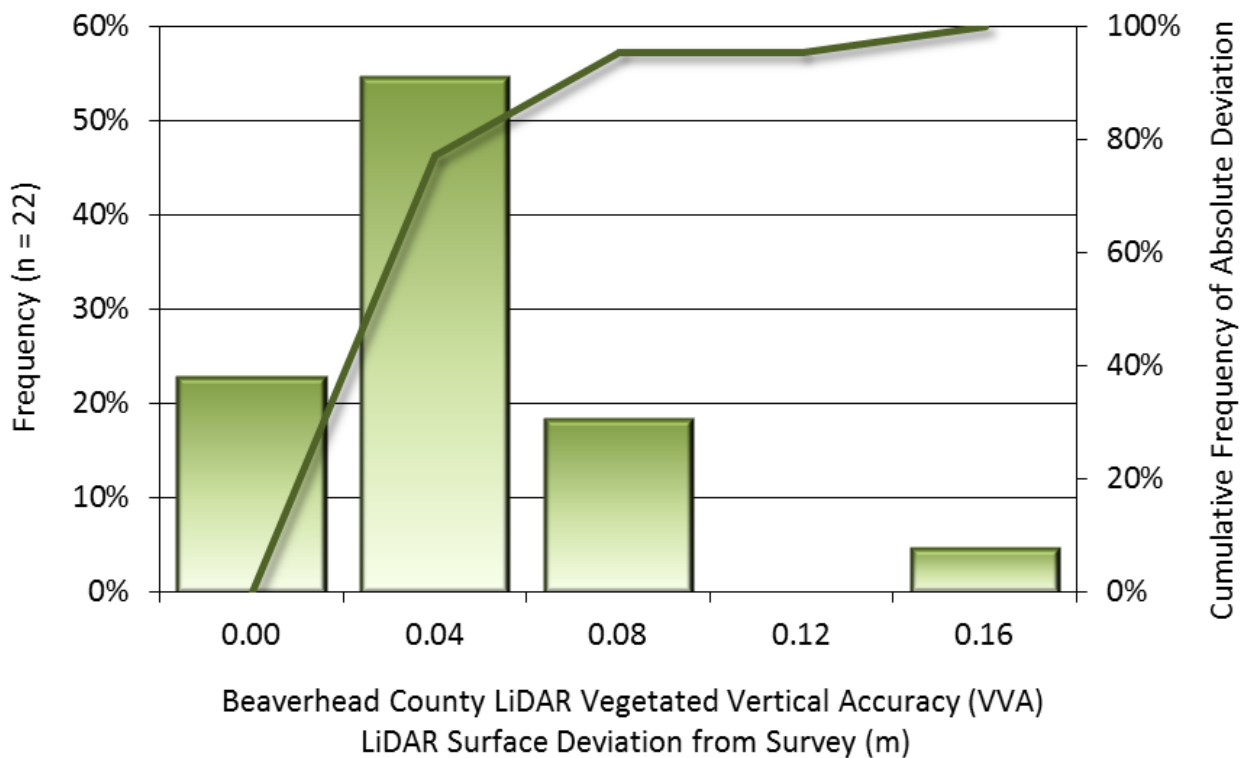


Figure 9: Frequency histogram for LiDAR surface deviation from all land cover class point values (VVA)

LiDAR Relative Vertical Accuracy

Relative vertical accuracy refers to the internal consistency of the data set as a whole: the ability to place an object in the same location given multiple flight lines, GPS conditions, and aircraft attitudes. When the LiDAR system is well calibrated, the swath-to-swath vertical divergence is low (<0.10 meters). The relative vertical accuracy was computed by comparing the ground surface model of each individual flight line with its neighbors in overlapping regions. The average (mean) line to line relative vertical accuracy for the Dillon AOI LiDAR project was 0.017 meters (Table 12, Figure 10).

Table 12: Relative accuracy results

Relative Accuracy	
Sample	31 surfaces
Average	0.017 m
Median	0.017 m
RMSE	0.017 m
Standard Deviation (1σ)	0.001 m
1.96σ	0.002 m

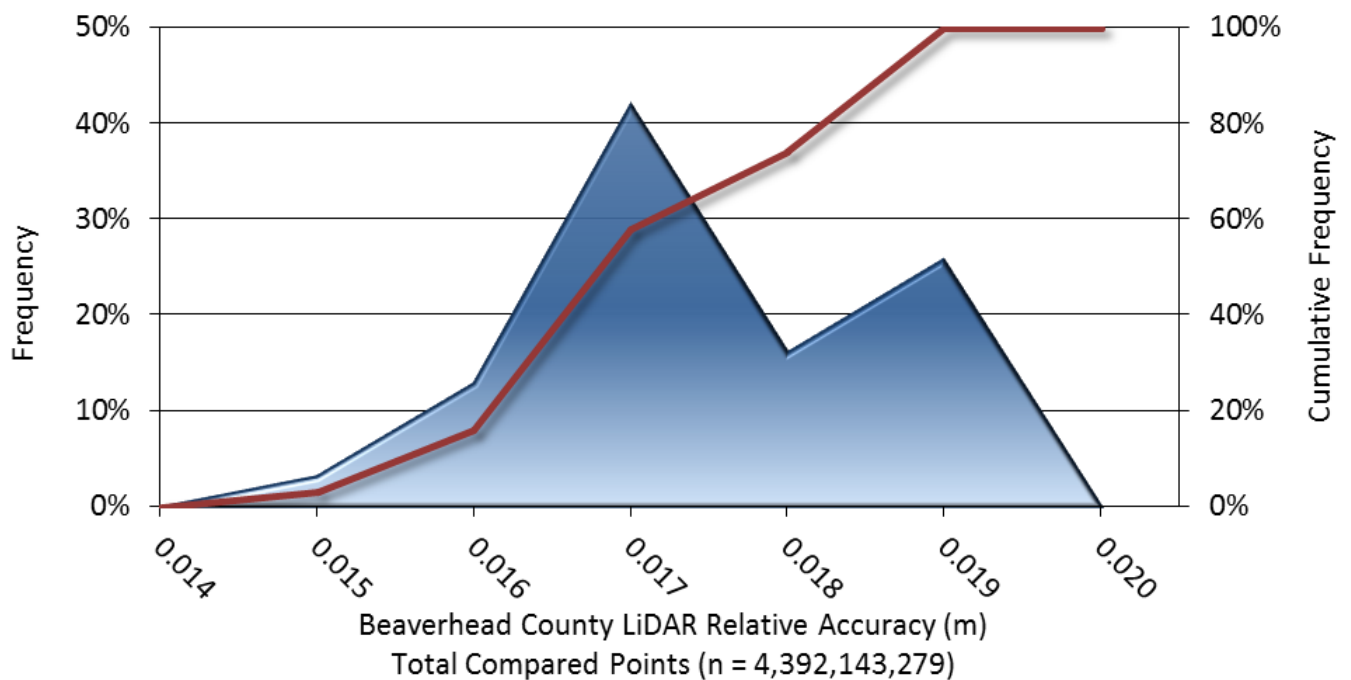


Figure 10: Frequency plot for relative vertical accuracy between flight lines



Figure 11: View looking northeast across a meandering river in the central part of the Dillon AOI. The image was created from the LIDAR bare earth model overlaid with the above-ground point cloud and USDA NAIP imagery.



Figure 12: The top image is a bare earth model, colored by elevation. It is view looking down and slightly north in the northern part of the Dillon AOI.

1-sigma (σ) Absolute Deviation: Value for which the data are within one standard deviation (approximately 68th percentile) of a normally distributed data set.

1.96 * RMSE Absolute Deviation: Value for which the data are within two standard deviations (approximately 95th percentile) of a normally distributed data set, based on the FGDC standards for Non-Vegetated Vertical Accuracy (NVA) reporting.

Accuracy: The statistical comparison between known (surveyed) points and laser points. Typically measured as the standard deviation (σ) and root mean square error (RMSE).

Absolute Accuracy: The vertical accuracy of LiDAR data is described as the mean and standard deviation (σ) of divergence of LiDAR point coordinates from ground survey point coordinates. To provide a sense of the model predictive power of the dataset, the root mean square error (RMSE) for vertical accuracy is also provided. These statistics assume the error distributions for x, y and z are normally distributed, and thus we also consider the skew and kurtosis of distributions when evaluating error statistics.

Relative Accuracy: Relative accuracy refers to the internal consistency of the data set; i.e., the ability to place a laser point in the same location over multiple flight lines, GPS conditions and aircraft attitudes. Affected by system attitude offsets, scale and GPS/IMU drift, internal consistency is measured as the divergence between points from different flight lines within an overlapping area. Divergence is most apparent when flight lines are opposing. When the LiDAR system is well calibrated, the line-to-line divergence is low (<10 cm).

Root Mean Square Error (RMSE): A statistic used to approximate the difference between real-world points and the LiDAR points. It is calculated by squaring all the values, then taking the average of the squares and taking the square root of the average.

Data Density: A common measure of LiDAR resolution, measured as points per square meter.

Digital Elevation Model (DEM): File or database made from surveyed points, containing elevation points over a contiguous area. Digital terrain models (DTM) and digital surface models (DSM) are types of DEMs. DTMs consist solely of the bare earth surface (ground points), while DSMs include information about all surfaces, including vegetation and man-made structures.

Intensity Values: The peak power ratio of the laser return to the emitted laser, calculated as a function of surface reflectivity.

Nadir: A single point or locus of points on the surface of the earth directly below a sensor as it progresses along its flight line.

Overlap: The area shared between flight lines, typically measured in percent. 100% overlap is essential to ensure complete coverage and reduce laser shadows.

Pulse Rate (PR): The rate at which laser pulses are emitted from the sensor; typically measured in thousands of pulses per second (kHz).

Pulse Returns: For every laser pulse emitted, the number of wave forms (i.e., echos) reflected back to the sensor. Portions of the wave form that return first are the highest element in multi-tiered surfaces such as vegetation. Portions of the wave form that return last are the lowest element in multi-tiered surfaces.

Real-Time Kinematic (RTK) Survey: A type of surveying conducted with a GPS base station deployed over a known monument with a radio connection to a GPS rover. Both the base station and rover receive differential GPS data and the baseline correction is solved between the two. This type of ground survey is accurate to 1.5 cm or less.

Post-Processed Kinematic (PPK) Survey: GPS surveying is conducted with a GPS rover collecting concurrently with a GPS base station set up over a known monument. Differential corrections and precisions for the GNSS baselines are computed and applied after the fact during processing. This type of ground survey is accurate to 1.5 cm or less.

Scan Angle: The angle from nadir to the edge of the scan, measured in degrees. Laser point accuracy typically decreases as scan angles increase.

Native LiDAR Density: The number of pulses emitted by the LiDAR system, commonly expressed as pulses per square meter.

APPENDIX A - ACCURACY CONTROLS

Relative Accuracy Calibration Methodology:

Manual System Calibration: Calibration procedures for each mission require solving geometric relationships that relate measured swath-to-swath deviations to misalignments of system attitude parameters. Corrected scale, pitch, roll and heading offsets were calculated and applied to resolve misalignments. The raw divergence between lines was computed after the manual calibration was completed and reported for each survey area.

Automated Attitude Calibration: All data were tested and calibrated using TerraMatch automated sampling routines. Ground points were classified for each individual flight line and used for line-to-line testing. System misalignment offsets (pitch, roll and heading) and scale were solved for each individual mission and applied to respective mission datasets. The data from each mission were then blended when imported together to form the entire area of interest.

Automated Z Calibration: Ground points per line were used to calculate the vertical divergence between lines caused by vertical GPS drift. Automated Z calibration was the final step employed for relative accuracy calibration.

LiDAR accuracy error sources and solutions:

Type of Error	Source	Post Processing Solution
GPS (Static/Kinematic)	Long Base Lines	None
	Poor Satellite Constellation	None
	Poor Antenna Visibility	Reduce Visibility Mask
Relative Accuracy	Poor System Calibration	Recalibrate IMU and sensor offsets/settings
	Inaccurate System	None
Laser Noise	Poor Laser Timing	None
	Poor Laser Reception	None
	Poor Laser Power	None
	Irregular Laser Shape	None

Operational measures taken to improve relative accuracy:

Low Flight Altitude: Terrain following was employed to maintain a constant above ground level (AGL). Laser horizontal errors are a function of flight altitude above ground (about 1/3000th AGL flight altitude).

Focus Laser Power at narrow beam footprint: A laser return must be received by the system above a power threshold to accurately record a measurement. The strength of the laser return (i.e., intensity) is a function of laser emission power, laser footprint, flight altitude and the reflectivity of the target. While surface reflectivity cannot be controlled, laser power can be increased and low flight altitudes can be maintained.

Reduced Scan Angle: Edge-of-scan data can become inaccurate. The scan angle was reduced to a maximum of $\pm 15^\circ$ from nadir, creating a narrow swath width and greatly reducing laser shadows from trees and buildings.

Quality GPS: Flights took place during optimal GPS conditions (e.g., 6 or more satellites and PDOP [Position Dilution of Precision] less than 3.0). Before each flight, the PDOP was determined for the survey day. During all flight times, a dual frequency DGPS base station recording at 1 second epochs was utilized and a maximum baseline length between the aircraft and the control points was less than 13 nm at all times.

Ground Survey: Ground survey point accuracy (<1.5 cm RMSE) occurs during optimal PDOP ranges and targets a minimal baseline distance of 4 miles between GPS rover and base. Robust statistics are, in part, a function of sample size (n) and distribution. Ground survey points are distributed to the extent possible throughout multiple flight lines and across the survey area.

50% Side-Lap (100% Overlap): Overlapping areas are optimized for relative accuracy testing. Laser shadowing is minimized to help increase target acquisition from multiple scan angles. Ideally, with a 50% side-lap, the nadir portion of one flight line coincides with the swath edge portion of overlapping flight lines. A minimum of 50% side-lap with terrain-followed acquisition prevents data gaps.

Opposing Flight Lines: All overlapping flight lines have opposing directions. Pitch, roll and heading errors are amplified by a factor of two relative to the adjacent flight line(s), making misalignments easier to detect and resolve.